



Stimulation strategies for absence seizures: targeted therapy of the focus in coupled thalamocortical model

Zhihui Wang · Qingyun Wang

Received: 16 November 2018 / Accepted: 5 March 2019 / Published online: 12 March 2019
© Springer Nature B.V. 2019

Abstract Motivated by the recent experimental findings that thalamic reticular nucleus (TRN) may be a pacemaker of absence seizures, we explore whether changes in the level of TRN activation can induce absence seizures by using a coupled thalamocortical model. We first simulate different firing states by considering the interaction of pathway between cortical excitatory pyramidal neuronal population (PY)–TRN and specific relay nucleus (SRN)–TRN. By simultaneously increasing the coupling strength of each of these pathways, we can reproduce the absence seizures, which indicates that epileptic seizures may be caused by activating the TRN. We further infer that the TRN may be an epileptogenic focus. Following this, different stimulation strategies, including deep brain stimulation, 1:0 coordinated reset stimulation (CRS) and 3:2 CRS, are applied in TRN. By qualitatively analyzing the efficacy of three different stimulation methods, we find that 3:2 CRS is a more effective and safe method to control absence seizures in the first compartment, for which we then further explore the impact of 3:2 CRS in the second compartment. The results show that the additional stimulation in the second compartment also can lead to a considerable decrease in the spike-and-wave discharges (SWD) oscillation region. Therefore, we conclude that TRN-3:2 CRS is an optimal electrical stimulation method for our modeling and simula-

tion studies. Furthermore, we hope that these numerical simulation results can provide some references for the treatment of real epilepsy patients in the future.

Keywords Absence seizures · Deep brain stimulation (DBS) · Coordinated reset stimulation (CRS) · Coupled thalamocortical model · Dynamical transition

1 Introduction

Epilepsy is a chronic neurological disease that affects over 65 million people around the world [1]. Absence seizures are featured by synchronous 2–4 Hz SWD in electroencephalography (EEG) recordings, accompanying a brief impairment of consciousness in seizures [2]. In particular, children with absence seizures often experience some potential dangers such as cognitive difficulties and reductions in memory and learning [3]. Polack et al. [4] found that SWD was initiated in the cortex. Some human recordings showed the possible involvement of the thalamus during absence seizures [5]. Since the cerebral cortex and thalamus are involved in the absence seizures, researchers constructed an intact cortico-thalamic–thalamocortical (CT–TC) circuit to obtain dynamical transition phenomena and corresponding biophysics mechanisms [6,7]. Once the balance in CT–TC circuit is broken, it will result in a series of nervous disorders such as Parkinson’s disease and epilepsy. The TRN is also located in CT–TC circuit. And in this circuit, the TRN receives excitatory gluta-

Z. Wang · Q. Wang (✉)
Department of Dynamics and Control, Beihang University,
Beijing 100191, China
e-mail: nmqingyun@163.com

matergic inputs from the thalamus and cerebral cortex and sends inhibitory projections to the SRN. TRN is regarded as a pacemaker of absence seizures. However, due to the complex connection between the thalamus and cerebral cortex, the potential mechanism on how the TRN regulates the epileptic seizures is not clarified.

Inhibitory signals play fundamental roles in regulating circuit mechanism and that originate from different GABAergic interneurons within the brain [8]. Parvalbumin (Pv) interneurons are expressed in some GABAergic interneurons, and some are expressed in TRN [9, 10]. Indeed, Pv interneurons could effectively control network excitability in previous experimental models of absence seizures [11]. However, in recent optogenetic studies, there are two conflicting viewpoints on the role of Pv interneurons in the regulation of absence seizures in TRN. The first viewpoint was that the optogenetic activation of Pv interneurons suppressed the epileptic seizures through a feed-forward inhibition [12, 13]. Nevertheless, the opposing viewpoint was that the optogenetic activation of Pv interneurons enhanced spontaneous ictal events in the epileptic seizures [14, 15]. Based on the contradiction, Sessolo et al. [16] put forward a selective activation role of Pv interneurons in mouse experiment with epilepsy. When Pv interneurons were distant from the focus of epileptic seizures, the Pv interneurons could prevent ictal propagation, whereas when Pv interneurons were near the focus, the Pv interneurons were hard to block ictal generation. Therefore, these complementary perspectives on Pv interneurons here open up a new angle of view for us to understand how the local suppression circuit can regulate and control the epileptic seizures.

It is estimated that one-third of epilepsy patients is difficult to achieve good control with anti-epileptic drugs [17]. Surgical resection may be a good treatment choice just for a minority of patients [18]. The remaining 30–40% adult patients keep refractory [19]. Thus, what is needed now is an alternative treatment for refractory patients [20]. DBS is a therapeutic method of minimally invasive neurosurgery, which sends electrical pulses to specific brain region through implanted electrodes. DBS treatment was widely applied in many clinical trials, animal studies and computational models. For example, Lehtimäki et al. [21] reported that a patient with refractory epilepsy was cured after applying DBS in the centromedian nucleus of the thalamus. In a rat model of temporal lobe epilepsy, the electrical stimulation of TRN effectively suppressed the propa-

gation of epilepsy [22]. Based on a biophysical mean field model, Wang et al. demonstrated that absence seizures can be eliminated by applying the DBS in TRN [23]. Recently, a new and emerging approach, CRS is designed to counteract abnormal neuronal synchrony by desynchronization [24]. CRS sends short pulse trains at different times to different neural populations involved in abnormal neuronal discharges [25]. Fan et al. utilized the CRS strategy to stimulate globus pallidus externa (GPe), subthalamic nucleus (STN) and globus pallidus interna (GPi), respectively. After applying the CRS, the whole Parkinson's neural network appeared desynchronization [26]. Similarly, CRS was also used to inhibit absence seizures in a macroscopic mean field model [27]. Compared to DBS, CRS can stimulate alternately multiple subcutaneous structures, reduce electrical damage of the brain and prevent some possible complications. Electrical stimulation acted on TRN in many animal experiments was used to suppress epileptic seizures [20, 28, 29]. Berdiev and Luijtelhaar [30] found that TRN stimulation in the WAG/Rij rat model inhibited the cortical synchronous activity. Pantojajiménez et al. reported that high-frequency stimulation (HFS)–TRN could interrupt abnormal brain oscillation and had an anti-epileptic effect in Male Wistar rats [31, 32]. However, it remains unknown how to select the optimal strategies of stimulation to TRN.

In order to study more realistic situations, spatially extended models were widely used to produce the spike–wave oscillations in the cortex [33, 34]. Taylor et al. [35] extended a single neural field model to thalamo-cortical network and found a reasonable stimulation could induce epileptic spike–wave discharges. From the whole connection process, the information flows along the compartment in one direction. The simple eight neuronal population model is a basic thalamo-cortical network model. Although the network is simple, studies [36] were proved that the simple network could make predictions for a larger network. Therefore, in order to simplify the model, we expand the single-compartment cortico-thalamic neural field model [37] to the coupled cortico-thalamic model, which is composed of two cortico-thalamic compartments with unidirectional connection configurations. Firstly, absence seizures can be induced through the combined effect of two important pathways. Combining previous studies [16] with our current exploration, we further infer the focal area of epilepsy. And then, we apply three different stimulation methods including DBS, 1:0 CRS and

3:2 CRS in the epileptogenic focus and compare and analyze qualitatively the efficacy among them. Finally, we find the optimal electrical stimulation method in our modeling and simulation studies.

2 Description of model and different stimulus strategies

As we know, some macroscopic dynamical phenomena including simple oscillation, low firing oscillation and SWD oscillation all can be simulated in the neural field model. Some studies indicated that abnormal neuronal oscillations in the cortico-thalamic circuit could induce the absence seizures [38,39]. Taylor et al. [37] improved a neuronal population model, reproduced the pathological SWD activity and investigated the effect of single pulse stimulation in epileptic seizures [40]. The original Taylor model contains four types of neuronal populations, which is shown in Fig. 1a. In subcortical SRN–TRN circuit, there are two types of neuronal

populations including TRN population and SRN population, respectively. TRN population is mainly comprised of inhibitory interneuronal population and SRN population is mainly comprised of excitatory neuronal population. The cerebral cortex includes the inhibitory interneuronal (IN) population and cortical excitatory pyramidal (PY) neuronal population [40,41], respectively. The round heads lines represent the inhibitory projections regulated by GABA_A receptors, and the arrowheads lines represent the excitatory projections regulated by glutamate receptors.

Spatially extended models for macroscopic epileptic seizures were studied in the cortex [33,34], where they explored how the cortico-cortical connectivities affected the whole model networks. However, thalamus as a part of the subcortical region was also verified to participate in the pathogenesis of absence seizures [39]. We do not consider the unidirectional connection from the cerebral cortex (I) to the thalamus (II) or from the thalamus (I) to the cerebral cortex (II) between compartment I and compartment II in our expanded model because the cerebral cortex and thalamus are two different structures. The original Taylor model is extended into a 2-compartment coupled model, which is shown in Fig. 1b. And the 2-compartment coupled model is enough to reveal some qualitative behaviors of epilepsy. Our macroscopic model combines a two-compartment coupled cortico-thalamic network to simulate absence seizures and dynamical transitions among different oscillation states. In general, the resulting coupled model equations can be defined as follows:

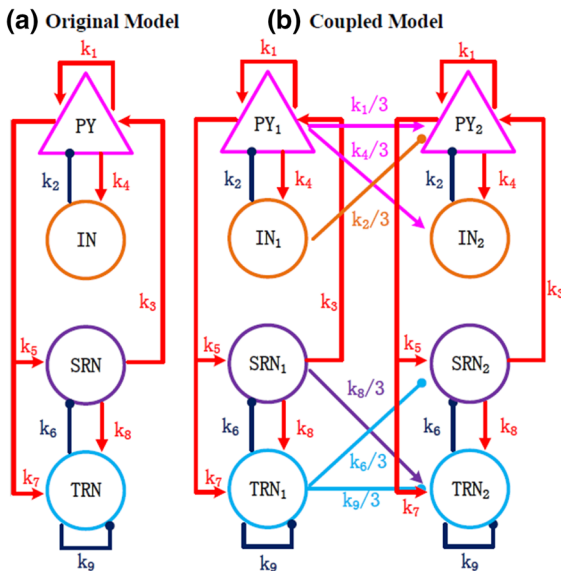


Fig. 1 Schematic diagrams of the original and coupled thalamocortical model. **a** Original model consists of four types of neuronal populations, which is composed of PY, IN in the cortex, SRN and TRN in the subcortical SRN–TRN circuit. **b** Coupled thalamocortical model. The arrowheads lines denote the excitatory projections mediated by glutamate receptors, and the round heads lines present the inhibitory projections mediated by GABA_A receptors. The short-range connection is considered in inter-compartment connections between two different coupled compartments

$$\frac{dPY_1}{dt} = (\varepsilon_{py} - PY_1 + k_1 F [PY_1] - k_2 F [IN_1] + k_3 F [SRN_1]) \tau_1, \tag{1}$$

$$\frac{dIN_1}{dt} = (\varepsilon_{in} - IN_1 + k_4 F [PY_1]) \tau_2, \tag{2}$$

$$\frac{dSRN_1}{dt} = (\varepsilon_{srn} - SRN_1 + k_5 F [PY_1] - k_6 G [TRN_1]) \tau_3, \tag{3}$$

$$\frac{dTRN_1}{dt} = (\varepsilon_{trn} - TRN_1 + k_7 F [PY_1] + k_8 G [SRN_1] - k_9 G [TRN_1]) \tau_4 + \beta_1(t) u(t), \tag{4}$$

$$\frac{dPY_2}{dt} = (\varepsilon_{py} - PY_2 + k_1 F [PY_2] - k_2 F [IN_2] + k_3 F [SRN_2]) \tau_1 + \frac{k_1}{3} F [PY_1] - \frac{k_2}{3} F [IN_1], \tag{5}$$

$$\frac{dIN_2}{dt} = (\varepsilon_{in} - IN_2 + k_4 F [PY_2]) \tau_2 + \frac{k_4}{3} F [PY_1], \tag{6}$$

$$\begin{aligned} \frac{dSRN_2}{dt} = & (\varepsilon_{sm} - SRN_2 + k_5 F [PY_2] \\ & - k_6 G [TRN_2]) \tau_3 - \frac{k_6}{3} G [TRN_1], \end{aligned} \quad (7)$$

$$\begin{aligned} \frac{dTRN_2}{dt} = & (\varepsilon_{tm} - TRN_2 + k_7 F [PY_2] + k_8 G [SRN_2] \\ & - k_9 G [TRN_2]) \tau_4 + \frac{k_8}{3} G [SRN_1] \\ & - \frac{k_9}{3} G [TRN_1] + \beta_2(t) u(t), \end{aligned} \quad (8)$$

where PY_i ($i = 1, 2$) and IN_i ($i = 1, 2$) are located in the cerebral cortex, which represents the pyramidal neuronal population and the inhibitory interneuronal population, respectively. And TRN_i ($i = 1, 2$) and SRN_i ($i = 1, 2$) are located in the thalamus, which represents the neuronal populations of the thalamic reticular nucleus and the specific relay nucleus, respectively. ε_{py} , ε_{in} , ε_{sm} , ε_{tm} are input parameters [33]. k_1, k_2, \dots, k_9 are the coupling strengths among different neuronal populations. $\tau_1, \tau_2, \tau_3, \tau_4$ are time scale parameters. $F[\cdot]$ and $G[\cdot]$ are activation functions [36], which are defined as follows:

$$F[x] = (1 / (1 + \varepsilon^{-x})), \quad (9)$$

$$G[y] = ay + b, \quad (10)$$

where $x = PY_i$ ($i = 1, 2$), IN_i ($i = 1, 2$), SRN_i ($i = 1, 2$), and TRN_i ($i = 1, 2$), and $y = SRN_i$ ($i = 1, 2$) and TRN_i ($i = 1, 2$). The parameters ε and a mean the steepness of two different activation functions, respectively. The parameter b is a constant. The axons of cortical excitatory PY neuronal population are long enough to affect the distant neuronal populations. Except for the axons of PY neuronal population, other axons are typically too short, and it is only possible to affect their adjacent areas. Therefore, there are three different inter-compartment connections including short-range connection, long-range connection and distant excitatory connection based on the distance between coupled two compartments. The corresponding connective strength k_i/m_k ($i = 1, 2, 4, 6, 8, 9$; $k = 1, 2, 3$) for the three inter-compartment connections also can be divided into k_i/m_1 ($m_1 = 3$), k_i/m_2 ($m_2 = 6$) and k_i/m_3 ($m_3 = 9$), respectively. We just consider two coupled compartments, which just can affect their adjacent areas in cerebral cortex and thalamus, respectively. Therefore, the short-range connection is applied in our model. And the parameter $k_i/3$ will be described as inter-compartment connection strength between two different coupled compartments. The

connection scheme of these equations is shown in Fig. 1b.

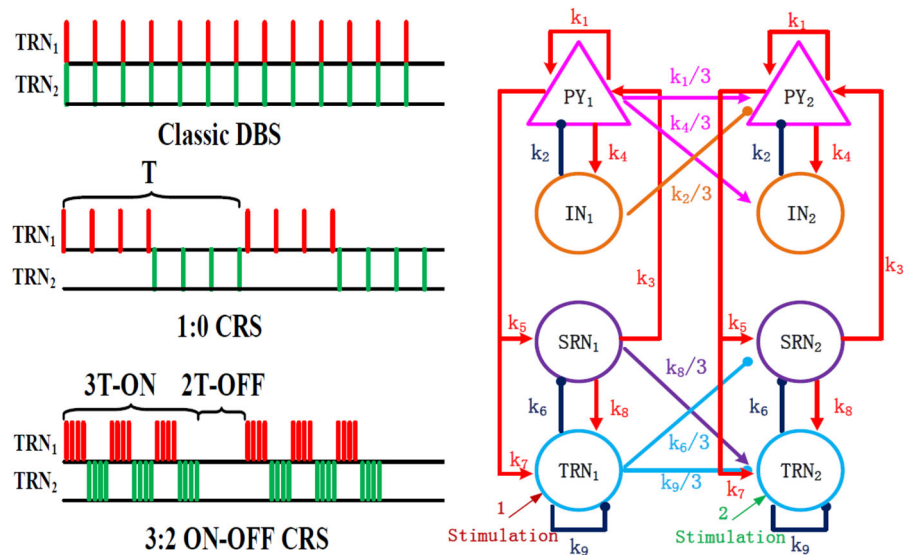
For simplicity, a sigmoid activation term $F[x] = (1 / (1 + \varepsilon^{-x}))$ in the thalamic subsystem is replaced by the linear function $G[x] = ax + b$. This is a reasonable approximation because the thalamus works well in the linear range of $F[x]$ for the SWD [37]. The qualitative agreement between the two different activation terms including sigmoid and linear functions has been displayed in the studies of Taylor et al. [40]. In addition, to explore the effect of different stimulation methods including TRN-DBS, TRN-1:0 CRS and TRN-3:2 CRS on SWD, we add stimulation control variables $u(t)$ and $I_{CRS}(t)$. The detailed schematic diagram is shown in Fig. 2. $u(t)$ represents the DBS control strategy, and $I_{CRS}(t)$ represents the CRS control strategy. DBS stimulates both TRN_1 and TRN_2 simultaneously. We use the 1:0 CRS strategy to stimulate TRN_1 and TRN_2 alternately, beginning with TRN_1 . However, we use the 3:2 CRS strategy firstly to stimulate TRN_1 and TRN_2 alternately for three cycles, also beginning with TRN_1 , and then stop stimulating TRN_1 and TRN_2 for two cycles.

A periodic step function can be used to well simulate DBS as follows [42]:

$$u(t) = \alpha \times H\left(\sin\left(\frac{2\pi}{\rho}\right)\right) \left(1 - H\left(\sin\left(\frac{2\pi(t+\delta)}{\rho}\right)\right)\right), \quad (11)$$

where parameter δ is a positive input pulse, which determines effective stimulus duration. Parameter α denotes the amplitude, and ρ denotes the stimulation period. H is Heaviside step function. The instantaneous frequencies f can be described as $1/\rho$, which can be found in previous studies [43]. The amplitude α and pulse width δ we used in our model were presented in previous experimental data [44, 45]. High-frequency stimulation was also proved to be effective in controlling absence seizures. For example, HFS (130 Hz) of the substantia nigra pars reticulata (SNr) in a genetic model of rats suppressed absence seizures [45]. Bilateral HFS of the subthalamic nuclei inhibited spontaneous absence seizures in rat models [46]. Based on the above studies, we choose stimulation amplitude $\alpha = 2$ mA, the positive input pulse $\delta = 1$ ms and frequency $f = 130$ Hz.

Fig. 2 Framework of the coupled thalamocortical model including different stimulation strategies. DBS stimulates TRN₁ and TRN₂ simultaneously. 1:0 CRS strategy stimulates TRN₁ and TRN₂ alternately. However, an integrated 3:2 CRS strategy firstly stimulates TRN₁ and TRN₂ alternately for three cycles and then stops stimulating TRN₁ and TRN₂ for two cycles



In our model, we activate two electrodes including TRN₁ and TRN₂, respectively. The $m:n$ ON–OFF CRS signal can be expressed as follows [47]:

$$I_{CRS}(t) = \beta_1(t)u(t) + \beta_2(t)u(t), \tag{12}$$

where subscripts 1 and 2 represent two kinds of stimulation microelectrodes. $\beta_1(t)$ and $\beta_2(t)$ represent index functions with respect to the time t . And the index functions at time point t are described as follows [47]:

$$\beta_k(t) (k = 1, 2) = \begin{cases} 0, & \text{the } k \text{ th electrode is closed} \\ 1, & \text{the } k \text{ th electrode is opened} \end{cases} \tag{13}$$

Therefore, Eqs. (11)–(13) jointly determine different stimulation methods for epileptogenic focus TRN₁ and TRN₂.

In order to compare the efficacy of three different stimulation strategies, we need to find a qualitative index to measure them. After adding stimulation, the first method should be to estimate the percentage reduction in absence seizures area. And then we also consider the energy saving and stimulation risk of machines and patients, respectively. Here, we introduce the root mean square (RMS) value of $I_{CRS}(t)$ and $u(t)$ to calculate the amount of electrical current stimuli, which are defined as follows [42]:

$$I_{RMS} = \frac{1}{\sqrt{N}} \| * \|_2, (* = I_{CRS}(t), u(t)), \tag{14}$$

where $I_{CRS}(t)$ and $u(t)$ represent the CRS and DBS currents, respectively. $\| * \|_2$ denotes the two-norm of $I_{CRS}(t)$ and $u(t)$. N is total time steps.

Table 1 Parameter values used in the computational model

Parameters	Value	Parameters	Value	Parameters	Value
ε_{py}	− 0.35	k_3	1	a	2.8
ε_{in}	− 3.4	k_4	4	b	0.5
ε_{srn}	− 2	k_5	3	α	2
ε_{trn}	− 5	k_6	0.6	f	130
k_1	1.8	k_9	0.2	δ	0.001
k_2	1.5	ε	250,000	τ_1	26
τ_2	32.5	τ_3	2.6	τ_4	2.6

Most parameters we used in our model are from original experimental data, which are used in previous studies [33, 34, 36, 40, 41]. The choice of parameters also is shown in Table 1. However, the connection parameters between coupled inter-compartment are estimated in numerical studies due to the lack of some corresponding experimental data. In order to obtain rich dynamical phenomena, some critical parameters including coupling strength k_7 and k_8 will be changed within a proper range. The MATLAB R2013a (MathWorks, USA) simulation environment is very flexible and is used to perform all of the numerical calculations in our model. The fixed temporal resolution of numerical integration is 0.25 ms. All the simulations are performed up to 18 seconds. The integration step is sufficiently small to ensure the numerical accuracy in our computational model. Using the standard fourth-order Runge–Kutta method, we solve the dynamical differen-

tial equations and analyze the corresponding dynamic properties [35,48,49].

3 Results

3.1 TRN may be a focus of absence seizures

As we know, TRN is comprised of inhibitory interneurons and plays the main role in adjusting and controlling physical motor [2]. Lewis et al found that TRN could induce rapid modulation of the local cortical state by using optogenetics and whole cortex electrophysiology [50]. Liu and Wang [2] used a computational model to explore the transition dynamics of generalized multiple epileptic seizures associated with thalamic reticular nucleus excitability. The inhibitory TRN was found to be a hub of the attentional system that gated thalamocortical signaling [51]. Therefore, it is generally believed that TRN is a pacemaker of absence seizures. However, the underlying mechanisms on how the TRN regulate the epilepsy activities are still unclear. Therefore, we focus on whether changes in the level of TRN activation can induce absence seizures. There are two main pathways for controlling the excitability of TRN; one is the excitatory synaptic coupling strength k_7 from PY to TRN, and the other is excitatory coupling strength k_8 in SRN–TRN pathway. We explore one-dimensional bifurcation analysis concerning the parameters k_7 and k_8 (see Fig. 3a, b), respectively. As we know, EEG data are collected by superimposing the firing activities of all neuronal populations in a local brain region. And in our model, the cerebral cortex includes the inhibitory interneuronal (IN) population and cortical excitatory pyramidal (PY) neuronal population. Therefore, by computing the mean field potential of excitatory and inhibitory neuronal populations $((PY+IN)/2)$, the firing activities of cortex can be better simulated in our computational model. In this section, we mainly consider and analyze the first compartment in our coupled field model, i.e., $(PY_1 + IN_1)/2$. Three different dynamical states can be obtained from bifurcation analysis, and corresponding time series are presented in Fig. 3(c1, c2, c3) and (d1, d2, d3). When the coupling strength k_7 is small, the activation level of TRN₁ will be relatively small. The firing of SRN₁ is hardly suppressed from the TRN₁ inhibition. The excitatory effect from SRN₁ on the cerebral cortex promotes cortical firing reaching the lowing firing state.

With the increase in k_7 , TRN₁ neurons slowly start inhibiting the activation of SRN₁. The activation level from SRN₁ to the cerebral cortex decreases. The firing activity becomes the simple oscillation state until k_7 increases to near 1.4. Finally, as coupling strength k_7 constantly increases, the TRN₁ completely suppresses the activation of SRN₁. And then, the system appears typical SWDs, which means the occurrence of absence seizures. The bifurcation analysis with respect to k_8 generates three different oscillation states including the lowing firing state, simple oscillation state and SWD oscillation state, and SWD oscillation region displays two pairs of minimums and maximums.

In accordance with the above description, we know that the pathways SRN₁-TRN₁ and PY₁-TRN₁ can regulate absence seizures, respectively. We further explore the joint regulation mechanism of these two pathways on the control of absence seizures. Firstly, the single-compartment computational model is analyzed. The two-dimensional state and dominant frequency analysis are plotted in (k_7, k_8) plane. Three different regions are shown in the whole plane in Fig. 4a, and different colors represent different regions. They are consistent with the states mentioned above. The green region III indicates SWD oscillation pattern, which represents the appearance of absence seizures. The regions II and I indicate the simple oscillation and lowing firing state, respectively. The SWD oscillation region in Fig. 4a comes within the 2–4-Hz frequency domain in Fig. 4b. The coupled two-compartment computational model is analyzed in Fig. 4c, d, respectively. Similarly, three different regions in different colors also can be found in the whole two-dimensional space. In general, the TRN₁ neuronal population receives excitatory signals from the SRN₁ neuronal population and the cortex. And then TRN₁ begins to regulate SRN₁ through an inhibitory pathway mediated by GABA_A receptors. In turn, the firing activity of SRN₁ can influence the dynamical characteristic of the cortical neuronal population and finally result in the appearance of different oscillation states. Comparing Fig. 4a, c, we find that Fig. 4c shows more SWD oscillation region. When the original model is extended to a simple eight neuronal population model, more pathological regions appear.

For the coupled two compartments computational model, when the coupling strength k_7 and k_8 are increased simultaneously in a proper range, epileptic seizures can be induced (see Fig. 4c). From the schematic diagram of the computational model,

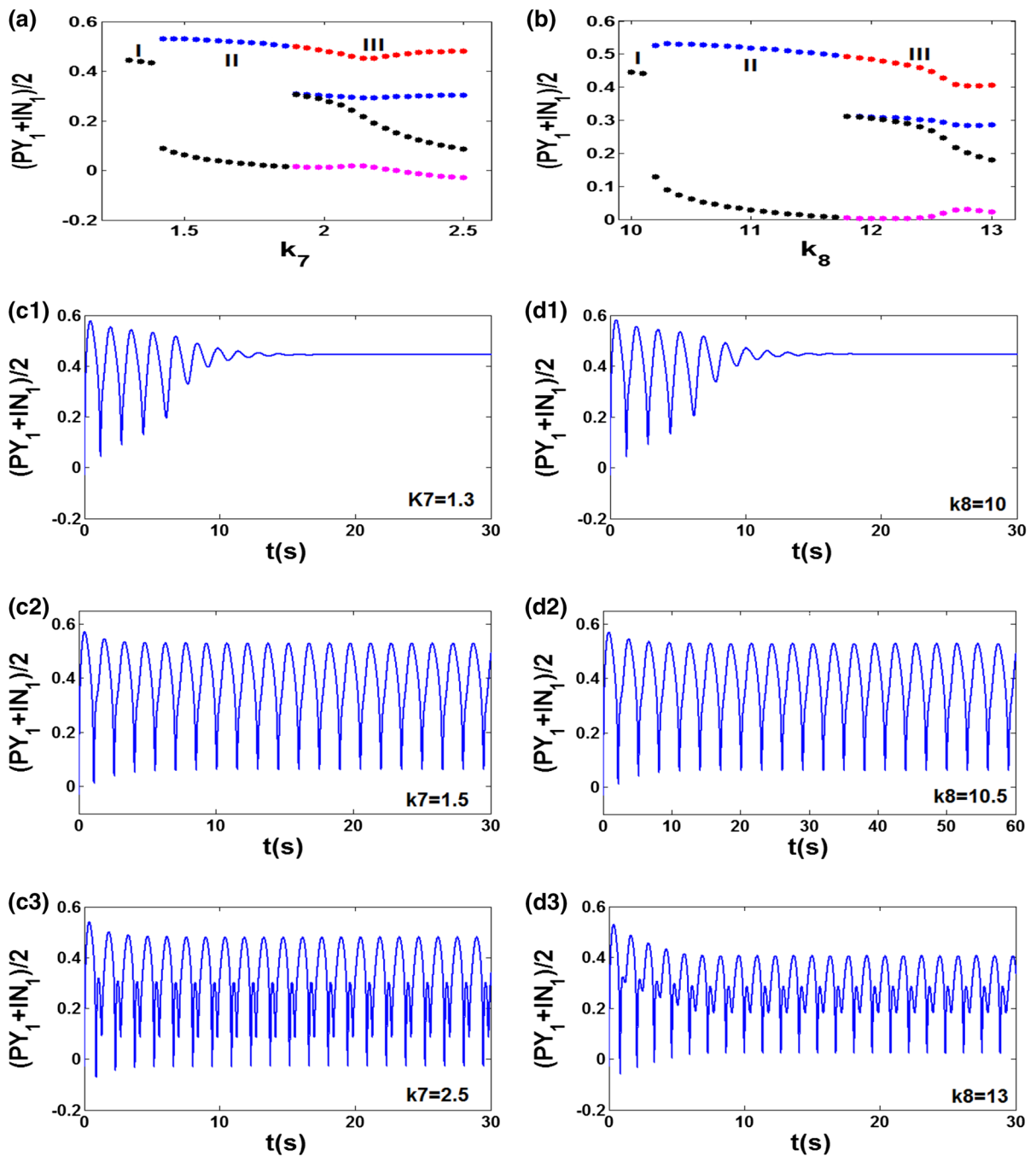
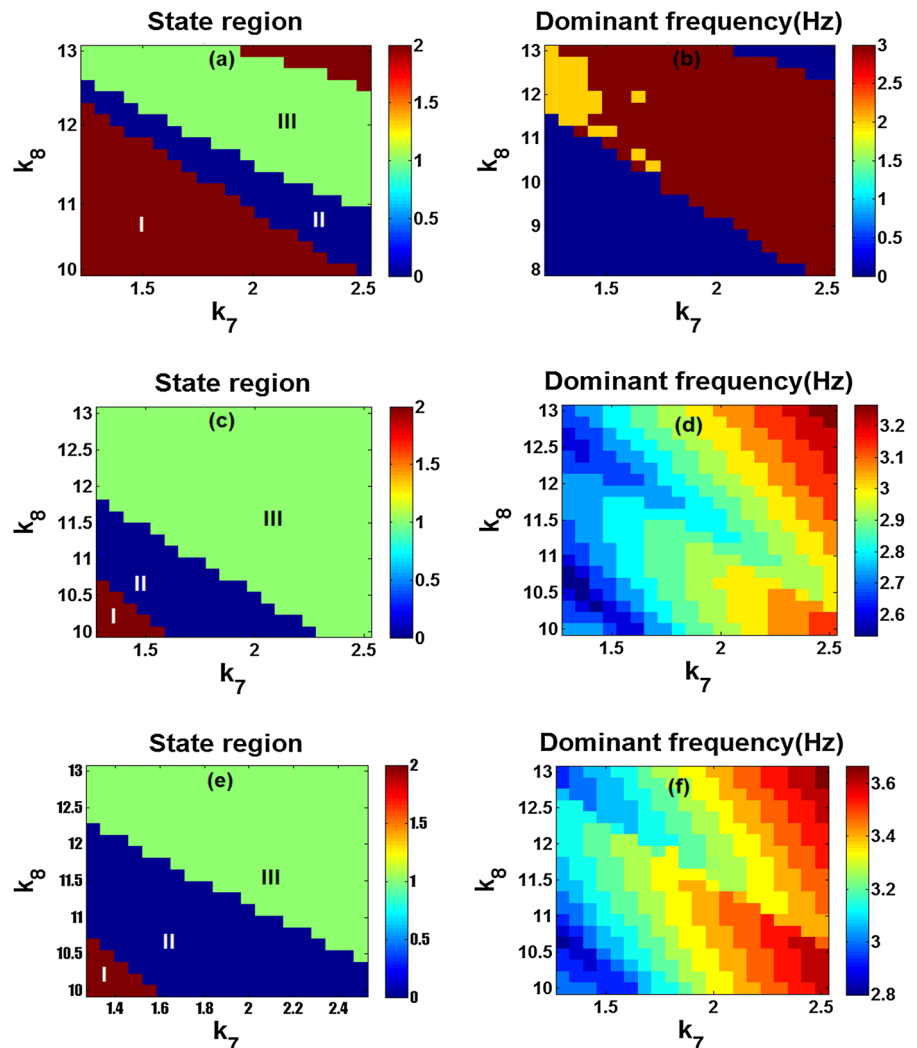


Fig. 3 Absence seizures induced by the coupling strength of PY–TRN and SRN–TRN pathways, respectively, in compartment I. **a** The bifurcation analysis of mean neuronal populations in the cortical network as a function of k_7 ($k_8 = 10.5$). **b** The bifurcation analysis of $(PY_1 + IN_1)/2$ as a function of k_8 ($k_7 = 1.5$). Here the coupling excitatory strength of PY–TRN pathway is represented as k_7 , and the coupling excitatory strength of SRN–TRN pathway

is expressed as k_8 . Three different dynamical oscillation regions including the low firing region (I), the simple oscillation region (II), and the SWD oscillation region (III) are demonstrated. **c, d** describe the time sequences of above three dynamical states. In this model, the variables $k_7 = 1.3$ (**c1**), $k_7 = 1.5$ (**c2**), $k_7 = 2.5$ (**c3**), and $k_8 = 10$ (**d1**), $k_8 = 10.5$ (**d2**), $k_8 = 13$ (**d3**) are set, respectively

Fig. 4 In the two-dimensional plane, dynamical state (a) and corresponding frequency analysis (b) are displayed in the single-compartment model, respectively. The green region III means SWD oscillation pattern, which represents the appearance of absence seizures. The blue region II and red region I mean the simple oscillation and lowing firing state, respectively. In the coupled compartment model, the dynamical state (c) and corresponding frequency analysis (d) are displayed in the compartment I, respectively. The dynamical state (e) and corresponding frequency analysis (f) are displayed by decreasing the activation of TRN. (Color figure online)



we know that when k_7 and k_8 are constant and increased, the activation degree of TRN_1 will be increased. Generally speaking, parvalbumin (Pv) interneurons are included in the inhibitory neurons of TRN_1 . Therefore, the activity of Pv interneurons in TRN_1 will also be enhanced. However, this activation leads to epileptic seizures in our model. Sessolo et al. found that Pv interneurons had a selective activation. When Pv interneurons were distant from the focus of epileptic seizures, the Pv interneurons could prevent ictal propagation, whereas when Pv interneurons were near the focus, the Pv interneurons were hard to block ictal generation [16]. Therefore, TRN_1 may be a focus of absence seizures. On the other hand, we appropriately adjust coupling strengths, input parameters and time scale parameters in order to keep the inputs to

TRN at a high level and maintain unchanged. The two-dimensional dynamical state (Fig. 4e) and corresponding frequency analysis (Fig. 4f) are plotted in (k_7, k_8) plane through artificially decreasing the activation of TRN . In contrast to the SWD region in Fig. 4c, we find that Fig. 4e shows a smaller SWD region. In other words, when we artificially decrease the activation of TRN and keep the inputs to TRN at a high level, the region of absence seizures has an apparent reduction. Combined with the results above, we can conclude that TRN_1 is very likely to be the focal area of epilepsy. Similarly, TRN_2 is also a possible epileptogenic focus. Therefore, three different stimulation methods are applied in the TRN_1 and TRN_2 , respectively, and explore whether they can suppress absence seizures effectively.

3.2 The effects of three different stimulation strategies acting on the TRN

Common epilepsy treatment, such as the medication, is the primary modality now. However, epilepsy cannot be cured completely, and most people need to continue to take medicine or accept other treatments [52]. There are some risks in surgical resection of epileptogenic foci [53]. Therefore, doctors have been trying several new treatments for epilepsy: DBS and CRS. However, it remains unknown how to select the optimal strategies of stimulation to TRN. In Sect. 3.1, we know that TRN including TRN_1 and TRN_2 may be the focal area of epilepsy. Based on the above conclusions, we use a coupled neural field model by applying three different stimulation strategies in TRN, respectively, and explore corresponding effects on the epileptic cortical dynamics. We mainly use the area of two parameters causing SWD as a measure for the effect of stimulation. The measurement method was widely used in previous studies. For example, Chen et al. [48] found that absence seizures could be controlled by exploring the state analysis and dominant frequency analysis between different coupling strengths. Fan and Wang [54] used the method to explore the decrease in SWD number through subthalamic nucleus deep brain stimulation (STN-DBS). By stimulating the coupled neuron, the control mechanism in real interactions of neurons was explored [55]. Therefore, the method used in this paper is a more reliable method. The framework of coupled field model including different stimulation distributions is shown in Fig. 2. The detailed strategies of DBS, 1:0 CRS and 3:2 CRS are also displayed in Fig. 2.

Based on the measurement method mentioned above, we investigate the possible effect of DBS in absence seizures. The two-dimensional dynamics state is plotted in (k_7, k_8) plane. Three different regions in different colors can be found in the whole two-dimensional space, which is shown in Fig. 5a. The green region III represents SWD oscillation state. As displayed in Fig. 5b, the pathological oscillation state in Fig. 5a comes within the 2–4 Hz frequency range. In contrast to the SWD region in Fig. 4c, we find that Fig. 5a shows a smaller SWD region. In other words, when we apply the DBS in TRN, the region of absence seizures has an obvious reduction. Next, we explore the impact of 1:0 CRS on TRN. Similarly, three different regions in different colors also can be found in the whole two-dimensional space, which is displayed in

Fig. 5c. And one of them is the SWD oscillation region. As shown in Fig. 5d, the pathological oscillation state in Fig. 5c comes within the 2–4 Hz frequency range. By comparison, we find the SWD region in Fig. 5c is smaller than the SWD region in Fig. 4c. Thus, 1:0 CRS acted on TRN can effectively control absence seizures. We finally investigate the effect of 3:2 CRS on TRN. We also use two-dimensional dynamical analysis to explore the changing processes of SWD oscillation state. As displayed in Fig. 5f, the pathological region in Fig. 5e falls into the 2–4-Hz frequency domain. By contrasting the SWD region in Figs. 4c and 5e, Fig. 5e has a smaller SWD region. The results show that 3:2 CRS also can effectively reduce the region of epileptic seizures. When the different stimulation methods are applied in TRN_1 , the stimulation may activate the TRN_1 or inhibit it. When we properly adjust the stimulation strategies and parameters, the stimulation can suppress the activation level of TRN_1 . The activation level of SRN_1 is slowly increased. The excitatory effect from SRN_1 on the cerebral cortex promotes cortical firing reaching the lowering firing state or simple oscillation state. Therefore, proper stimulation method is beneficial to the control of absence seizures. However, how to choose the optimal stimulation strategy is still unknown.

For a clearer recognizing and comparing the effect of the three stimulation methods, we measure several qualitative indexes, which are displayed in Fig. 6. The crimson bars represent electric current expenditure, and the dark blue bars mean the percentage reduction in absence seizures area after adding stimulation. From Fig. 6, we know DBS has the best effect on control seizures. The 3:2 CSR acted on TRN also can effectively reduce the disease areas, and the result is similar to that of 1:0 CRS. Meanwhile, Fig. 6 illustrates that the 3:2 CRS uses the least amount of stimulation current; however, the DBS uses the most amount of stimulation current on the system consume. The excessive use of current may lead to some bad influences on the human brain. And the single stimulation target and continuous strong stimuli both also might damage the surrounding brain tissue. Although the effect of DBS on controlling absence seizures is little stronger than that of 3:2 CRS, DBS might cause damaging side effects or complications. Therefore, we are more likely to choose 3:2 CRS and 1:0 CRS for security reasons. By contrasting the result of 3:2 CRS and 1:0 CRS, we find that they have a similar effect on reducing SWD oscillation region.

Fig. 5 Comparison diagrams among three different stimulation strategies in compartment I. **a, b** Two-dimensional dynamical evolution and corresponding frequency pcolor are displayed through adding DBS, respectively. **c, d** Dynamical evolution and corresponding frequency pcolor are plotted through adding 1:0 CRS, respectively. **e, f** Dynamical evolution and corresponding frequency pcolor are plotted through adding 3:2 CRS, respectively. Here we choose the same stimulation parameters, which include amplitude $\alpha = 2$ mA, the positive input pulse $\delta = 0.001$ s and frequency $f = 130$ Hz in these three stimulation methods

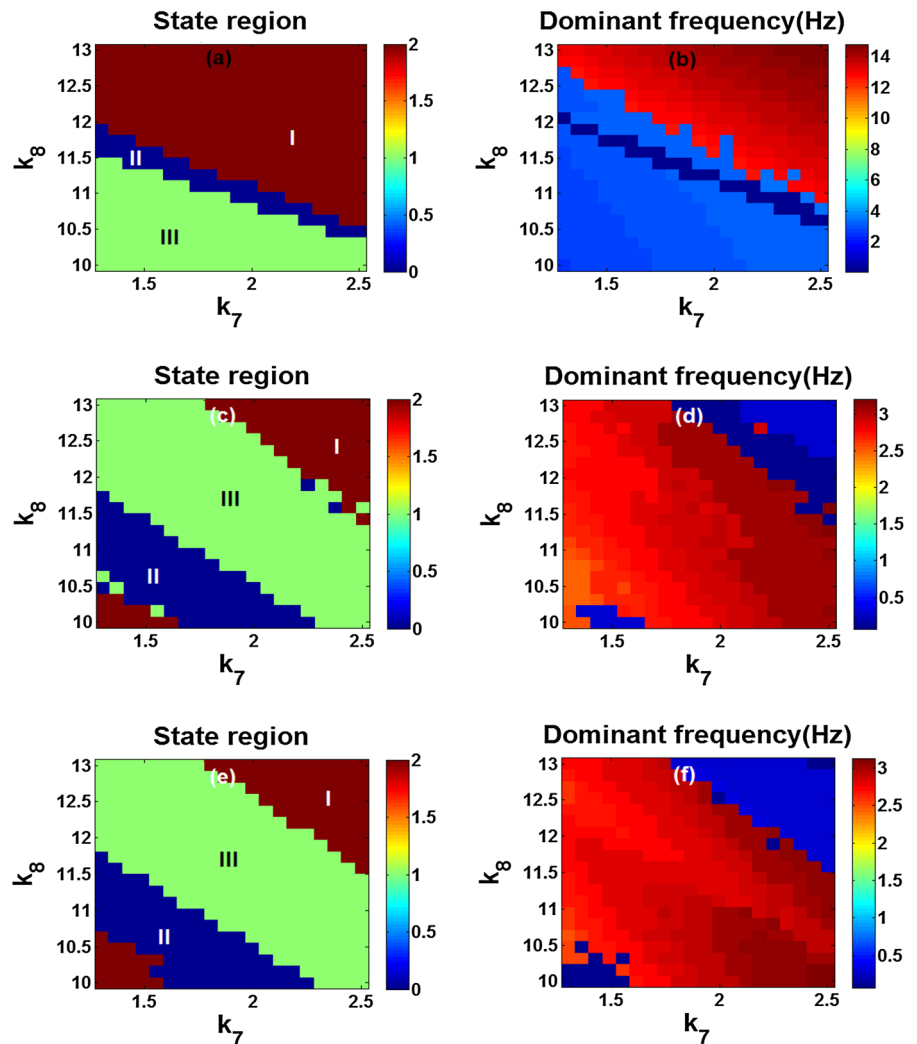
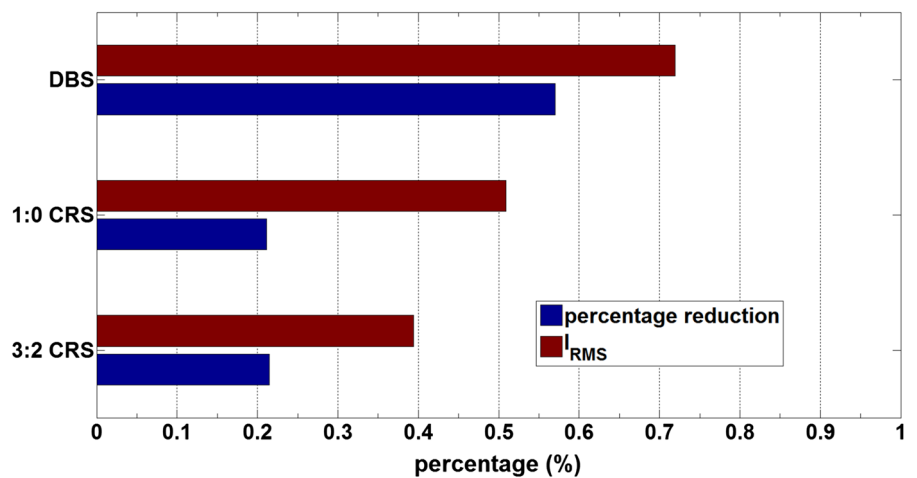


Fig. 6 Effect of DBS, 1:0 CRS and 3:2 CRS on the absence seizures in compartment I. The crimson bars represent electric current expenditure, and the dark blue bars mean the percentage reduction in absence seizures area after adding the stimulation. (Color figure online)



Nevertheless, the 3:2 CRS uses the less amount of stimulation current than 1:0 CRS. Therefore, 3:2 CRS is a relatively effective and safe method on control absence seizures.

3.3 The state changes from $PY_1 + IN_1$ to $PY_2 + IN_2$

In our model, we mainly consider 2 compartments of thalamocortical network. Therefore, the exploration of compartment II is also crucial and necessary. Combined with the results of Sect. 3.2, we will attempt to explore the 3:2 CRS strategy that focuses on compartment II in this section.

We first analyze the evolution of time courses of mean neuronal populations in cortex from compartment I to compartment II without stimulations. And each single compartment displays the normal state as $k_7 = 1.4$ and $k_8 = 10$, respectively. As shown in Fig. 7a, b, the first compartment is low firing state and the second compartment is simple oscillation state. With the increase in coupling coefficients k_7 and k_8

simultaneously, the compartment II first appears SWD oscillation state. As shown in Fig. 7c, d, the first compartment is simple oscillation activity and the second compartment is SWD oscillation activity. When we further increase the coupling parameters k_7 and k_8 , the compartment I starts to appear SWD oscillation state, and the compartment II still keeps pathological state (see Fig. 7e, f). Therefore, when the coupling strengths k_7 and k_8 are changed within a reasonable range, three different discharge patterns all can be showed in compartments I and II. The emphasis is on the appearance of absence seizures through enhancing the coupling strength of two pathways. Under the same parameters, we continue to explore the possible impact of 3:2 CRS. As shown in Fig. 8a, b, each single compartment displays the simple state as $k_7 = 1.4$ and $k_8 = 10$, respectively. With the coupling coefficients k_7 and k_8 being increased continually, there are no changes in the oscillation states in compartments I and II. They also display the simple oscillation state, which is shown in Fig. 8c, d. As further increasing the coupling parameters k_7 and

Fig. 7 Evolution of time courses of mean neuronal populations in cortex from compartment I to compartment II without stimulations. The blue line represents the time series in compartment I, and the red line represents the time series in compartment II. We choose several special parameters to observe the phenomena. When $k_7 = 1.4$ and $k_8 = 10$, the low firing state (a) in compartment I spreads into simple oscillation state (b) in compartment II; when $k_7 = 1.8$ and $k_8 = 10.5$, the simple oscillation (c) in compartment I spreads into SWD oscillation state (d) in compartment II; when $k_7 = 2.4$, $k_8 = 12.5$, the compartments I and II both show the SWD oscillation state (e, f). (Color figure online)

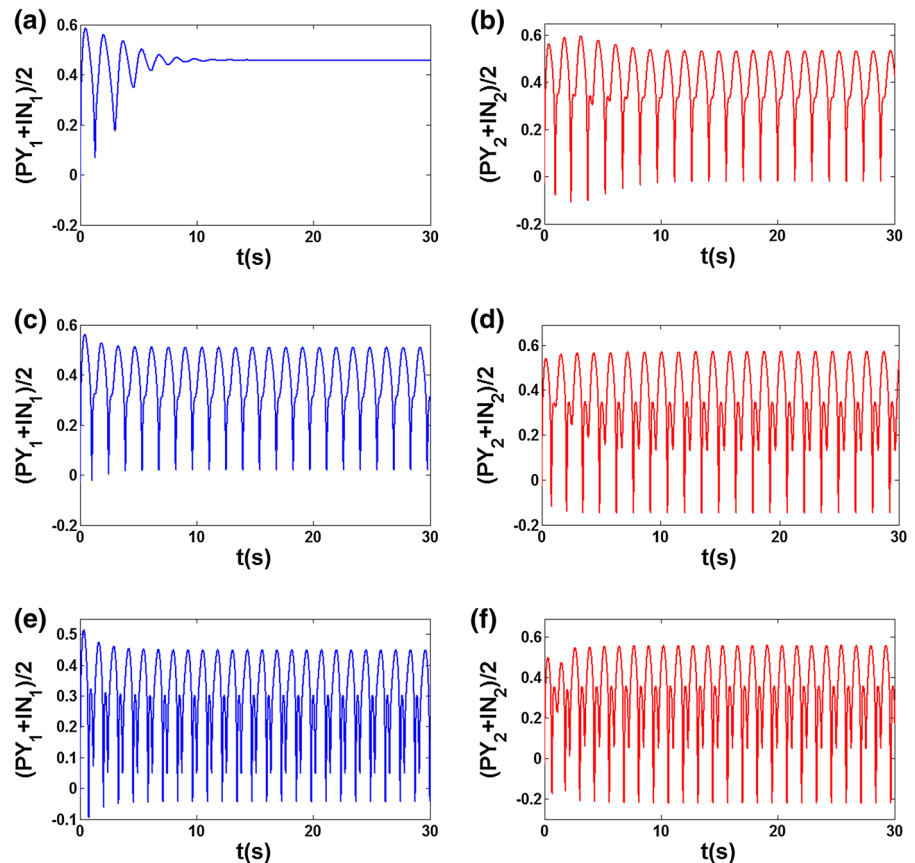


Fig. 8 Evolution of time courses of mean neuronal populations in cortex from compartment I to compartment II under the 3:2 CRS. The values of parameters including k_7 and k_8 are consistent with Fig. 7. The pathological SWD state all disappears in compartment I and compartment II. The normal oscillation states include the simple oscillation (a–d, f) and the low firing state (e)

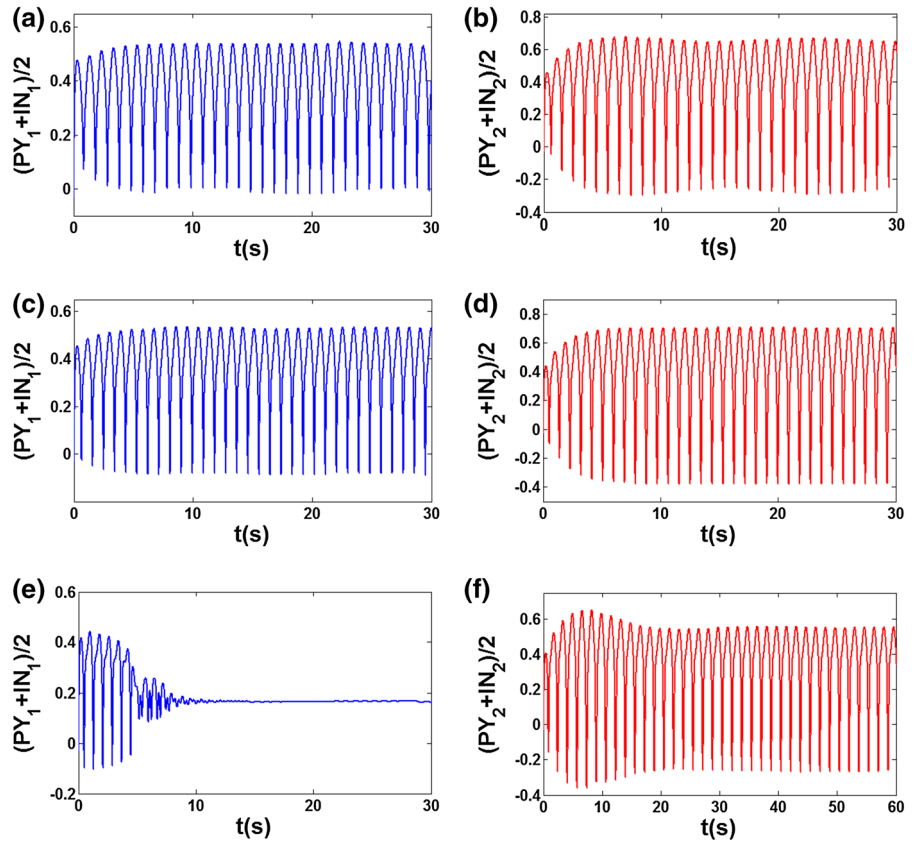
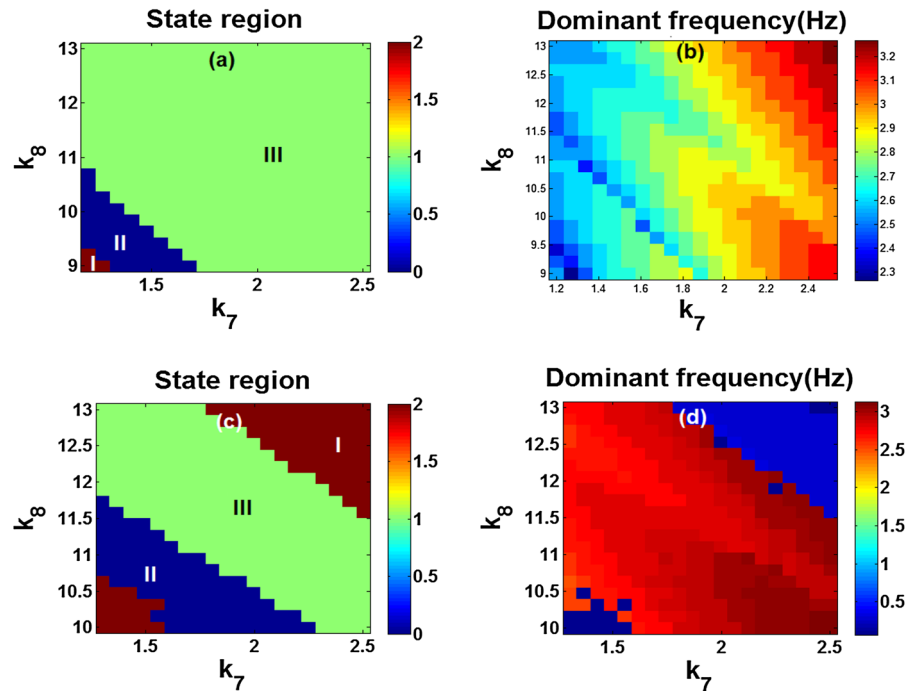


Fig. 9 Comparison diagrams in compartment II. **a, b** In the two-dimensional plane, dynamical state and corresponding frequency analysis are displayed, respectively. **c, d** Two-dimensional dynamical state and corresponding frequency analysis are plotted through adding 3:2 CRS, respectively. The green region III means SWD oscillation pattern. The regions II and I represent the simple oscillation state and lowering firing state, respectively. (Color figure online)



k_8 , the compartment I first becomes low firing state, and the compartment II still keeps simple oscillation state (Fig. 8e, f).

After the addition of stimulation, the epileptic discharges of compartments I and II both disappear. In particular, compartment II can always maintain normal firing oscillation state. Therefore, it is demonstrated that 3:2 CRS is effective in the treatment of absence seizures.

In the next, we mainly explore the second compartment. We first plot the two-dimensional bifurcation and dominant frequency analysis in (k_7, k_8) plane without stimulation. Three different regions can be found in the whole two-dimensional space, which is shown in Fig. 9a. The green region III represents SWD oscillation state. As displayed in Fig. 9b, the SWD oscillation state in Fig. 9a comes within the 2–4 Hz frequency range. By contrast, the SWD oscillation region in compartment II (Fig. 9a) is slightly larger than that in compartment I (Fig. 4c). After adding the stimulation, the two-dimensional dynamics state is still plotted in (k_7, k_8) plane. As displayed in Fig. 9d, the SWD oscillation state in Fig. 9c also comes within the 2–4 Hz frequency range. By contrasting the SWD region in Fig. 9a, c, we find Fig. 9c has a smaller SWD region. It means that the epileptic seizures can be controlled by stimulation in compartment II. Therefore, 3:2 CRS has a significant inhibitory effect on the second compartment.

4 Conclusion

In this paper, we explore whether changes in the level of TRN activation can induce absence seizures. Two principal pathways are proposed to control the TRN activation level in our model: one is the excitatory coupling strength k_7 in pathway PY–TRN and the other is the excitatory coupling strength k_8 in pathway SRN–TRN. Absence epilepsy activity appears when the coupling strengths are increased simultaneously within a certain scope, which indicates that in our computational model, epileptic seizures are caused by activating the TRN population. According to Sect. 3.1, we infer that the TRN is very likely to be the focal zone of epilepsy. Therefore, we apply three different stimulation methods including DBS, 1:0 CRS and 3:2 CRS in TRN to find an optimal control strategy. The evolution of mean neuronal populations in the first compartment of the

cortex is considered. Through qualitatively comparing and analyzing the efficacy among the three stimulation methods, we find that DBS displays its most effective ability on controlling seizures. The application of the 3:2 CRS in TRN potentially leads to critical reductions in the disease areas, and the 1:0 CRS application also produces similar results. Considering the consumption, the 3:2 CRS utilizes the least stimulation current. Yet DBS corresponds to the most stimulation current and stimulates both TRN₁ and TRN₂, simultaneously; therefore, DBS might increase the risk of side effects. Since the 3:2 CRS takes less stimulation current than the 1:0 CRS, the 3:2 CRS is a more effective and safer method on controlling absence seizures for the first compartment. On the other hand, we explore the state changes in the second compartment. Following the addition of stimulation, epileptic discharges in both compartments I and II disappear, and especially in the compartment II, which maintains a normal firing oscillation. Furthermore, absence seizures region in compartment II has a considerable reduction when the 3:2 CRS is applied to the TRN. Accordingly, we conclude that the TRN-3:2 CRS can provide a better method for the control of absence seizures in our model.

Acknowledgements This work was supported by the National Natural Science Foundation of China (Grant No. 11772019).

Compliance with ethical standards

Conflict of interest The authors declare that they have no conflict of interest.

Human and animals rights This article does not contain any studies with human participants or animals performed by any of the authors.

References

1. Barad, Z., Grattan, D.R., Leitch, B.: NMDA receptor expression in the thalamus of the stargazer model of absence epilepsy. *Sci. Rep.* **7**, 42926 (2017)
2. Liu, S., Wang, Q.: Transition dynamics of generalized multiple epileptic seizures associated with thalamic reticular nucleus excitability: a computational study. *Commun. Nonlinear Sci. Numer. Simul.* **52**, 203–213 (2017)
3. Guerrini, R., Melani, F., Brancati, C., et al.: Dysgraphia as a mild expression of dystonia in children with absence epilepsy. *PLoS ONE* **10**(7), e0130883 (2015)
4. Polack, P.O., Guillemain, I., Hu, E., et al.: Deep layer somatosensory cortical neurons initiate spike-and-wave discharges in a genetic model of absence seizures. *J. Neurosci.* **27**(24), 6590–6599 (2007)

5. Steriade, M., Contreras, D.: Spike-wave complexes and fast components of cortically generated seizures. I. Role of neocortex and thalamus. *J. Neurophysiol.* **80**(3), 1439–1455 (1998)
6. Liu, Z., Vergnes, M., Depaulis, A., et al.: Involvement of intrathalamic GABA_B neurotransmission in the control of absence seizures in the rat. *Neuroscience* **48**(1), 87–93 (1992)
7. Liu, Z., Vergnes, M., Depaulis, A., et al.: Evidence for a critical role of GABAergic transmission within the thalamus in the genesis and control of absence seizures in the rat. *Brain Res.* **545**(1–2), 1–7 (1991)
8. Markram, H., Toledo-Rodriguez, M., Wang, Y., et al.: Interneurons of the neocortical inhibitory system. *Nat. Rev. Neurosci.* **5**(10), 793 (2004)
9. Adotevi, N.K., Leitch, B.: Alterations in AMPA receptor subunit expression in cortical inhibitory interneurons in the epileptic stargazer mutant mouse. *Neuroscience* **339**, 124–138 (2016)
10. Mineff, E.M., Weinberg, R.J.: Differential synaptic distribution of AMPA receptor subunits in the ventral posterior and reticular thalamic nuclei of the rat. *Neuroscience* **101**(4), 969–982 (2000)
11. Trevelyan, A.J., Sussillo, D., Watson, B.O., et al.: Modular propagation of epileptiform activity: evidence for an inhibitory veto in neocortex. *J. Neurosci.* **26**(48), 12447–12455 (2006)
12. Cammarota, M., Losi, G., Chiavegato, A., et al.: Fast spiking interneuron control of seizure propagation in a cortical slice model of focal epilepsy. *J. Physiol.* **591**(4), 807–822 (2013)
13. Schevon, C.A., Weiss, S.A., McKhann Jr., G., et al.: Evidence of an inhibitory restraint of seizure activity in humans. *Nat. Commun.* **3**, 1060 (2012)
14. Shiri, Z., Manseau, F., Lévesque, M., et al.: Interneuron activity leads to initiation of low-voltage fast-onset seizures. *Ann. Neurol.* **77**(3), 541–546 (2015)
15. Yekhle, L., Breschi, G.L., Lagostena, L., et al.: Selective activation of parvalbumin- or somatostatin-expressing interneurons triggers epileptic seizure-like activity in mouse medial entorhinal cortex. *J. Neurophysiol.* **113**(5), 1616–1630 (2014)
16. Sessolo, M., Marcon, I., Bovetti, S., et al.: Parvalbumin-positive inhibitory interneurons oppose propagation but favor generation of focal epileptiform activity. *J. Neurosci.* **35**(26), 9544–9557 (2015)
17. Kwan, P., Brodie, M.J.: Early identification of refractory epilepsy. *N. Engl. J. Med.* **342**(5), 314–319 (2000)
18. Engel, J., Wiebe, S., French, J., et al.: Practice parameter: temporal lobe and localized neocortical resections for epilepsy. *Epilepsia* **44**(6), 741–751 (2003)
19. Kwan, P., Arzimanoglou, A., Berg, A.T., et al.: Definition of drug resistant epilepsy: consensus proposal by the ad hoc Task Force of the ILAE Commission on Therapeutic Strategies. *Epilepsia* **51**(6), 1069–1077 (2010)
20. Pantoja-Jiménez, C.R., Magdaleno-Madrigal, V.M., Almazán-Alvarado, S., et al.: Anti-epileptogenic effect of high-frequency stimulation in the thalamic reticular nucleus on PTZ-induced seizures. *Brain Stimul.* **7**(4), 587–594 (2014)
21. Lehtimäki, K., Långsjö, J.W., Ollikainen, J., et al.: Successful management of super-refractory status epilepticus with thalamic deep brain stimulation. *Ann. Neurol.* **81**(1), 142–146 (2017)
22. Nanobashvili, Z., Chachua, T., Nanobashvili, A., et al.: Suppression of limbic motor seizures by electrical stimulation in thalamic reticular nucleus. *Exp. Neurol.* **181**(2), 224–230 (2003)
23. Wang, Z., Wang, Q.: Eliminating absence seizures through the deep brain stimulation to thalamus reticular nucleus. *Front. Comput. Neurosci.* **11**, 22 (2017)
24. Zeitler, M., Tass, P.A.: Anti-kindling induced by two-stage coordinated reset stimulation with weak onset intensity. *Front. Comput. Neurosci.* **10**(154), (2016)
25. Zeitler, M., Tass, P.A.: Augmented brain function by coordinated reset stimulation with slowly varying sequences. *Front. Syst. Neurosci.* **9**, 49 (2015)
26. Fan, D., Wang, Q.: Improving desynchronization of parkinsonian neuronal network via triplet-structure coordinated reset stimulation. *J. Theor. Biol.* **370**, 157–170 (2015)
27. Wang, Z.H., Wang, Q.Y.: Effect of the coordinated reset stimulations on controlling absence seizure. *Sci. China Technol. Sci.* **60**(7), 985–994 (2017)
28. Dow, R.S., Fernández-Guardiola, A., Manni, E.: The influence of the cerebellum on experimental epilepsy. *Electroencephalogr. Clin. Neurophysiol.* **14**(3), 383–398 (1962)
29. Mirski, M.A., Rossell, L.A., Terry, J.B., et al.: Anticonvulsant effect of anterior thalamic high frequency electrical stimulation in the rat. *Epilepsy Res.* **28**(2), 89–100 (1997)
30. Berdiev, R.K., Luijtelar, G.V.: Cholinergic stimulation of the nucleus basalis of Meynert and reticular thalamic nucleus affects spike-and-wave discharges in WAG/Rij rats. *Neurosci. Lett.* **463**(3), 249–253 (2009)
31. Pantojajiménez, C.R., Magdaleno-Madrigal, V.M., Almazán-Alvarado, S., et al.: Anti-epileptogenic effect of high-frequency stimulation in the thalamic reticular nucleus on PTZ-induced seizures. *Brain Stimul.* **7**(4), 587–594 (2014)
32. Fisher, R., Salanova, V., Witt, T., et al.: Electrical stimulation of the anterior nucleus of thalamus for treatment of refractory epilepsy. *Epilepsia* **51**(5), 899–908 (2010)
33. Taylor, P.N., Baier, G.: A spatially extended model for macroscopic spike-wave discharges. *J. Comput. Neurosci.* **31**(3), 679–684 (2011)
34. Goodfellow, M., Schindler, K., Baier, G.: Intermittent spike-wave dynamics in a heterogeneous, spatially extended neural mass model. *Neuroimage* **55**(3), 920–932 (2011)
35. Taylor, P.N., Baier, G., Cash, S.S., et al.: A model of stimulus-induced epileptic spike-wave discharges. In: 2013 IEEE Symposium on Computational Intelligence, Cognitive Algorithms, Mind, and Brain (CCMB), pp. 53–59. IEEE (2013)
36. Yan, B., Li, P.: An integrative view of mechanisms underlying generalized spike-and-wave epileptic seizures and its implication on optimal therapeutic treatments. *PLoS ONE.* **6**(7), e22440 (2011)
37. Taylor, P.N., Wang, Y., Goodfellow, M., et al.: A computational study of stimulus driven epileptic seizure abatement. *PLoS ONE* **9**(12), e114316 (2014)
38. Evangelista, E., Bénar, C., Bonini, F., et al.: Does the thalamo-cortical synchrony play a role in seizure termination? *Front. Neurol.* **6**, 192 (2015)
39. Moeller, F., Muthuraman, M., Stephani, U., et al.: Representation and propagation of epileptic activity in absences

- and generalized photoparoxysmal responses. *Human Brain Map.* **34**(8), 1896–1909 (2013)
40. Neal, T.P., Wang, Y., Marc, G., et al.: A computational study of stimulus driven epileptic seizure abatement. *PLoS ONE* **9**(12), e114316 (2014)
 41. Taylor, P.N., Thomas, J., Sinha, N., et al.: Optimal control based seizure abatement using patient derived connectivity. *Front. Neurosci.* **9**(9), 202 (2015)
 42. Ellis, T.L., Stevens, A.: Deep brain stimulation for medically refractory epilepsy. *Neurosurg. Focus* **25**(3), E11 (2008)
 43. McConnell, G.C., So, R.Q., Hilliard, J.D., et al.: Effective deep brain stimulation suppresses low-frequency network oscillations in the basal ganglia by regularizing neural firing patterns. *J. Neurosci.* **32**(45), 15657–15668 (2012)
 44. Benazzouz, A., Piallat, B., Pollak, P., et al.: Responses of substantia nigra pars reticulata and globus pallidus complex to high frequency stimulation of the subthalamic nucleus in rats: electrophysiological data. *Neurosci. Lett.* **189**(2), 77–80 (1995)
 45. Feddersen, B., Vercueil, L., Noachtar, S., et al.: Controlling seizures is not controlling epilepsy: a parametric study of deep brain stimulation for epilepsy. *Neurobiol. Dis.* **27**(3), 292–300 (2007)
 46. Vercueil, L., Benazzouz, A., Deransart, C., et al.: High-frequency stimulation of the sub-thalamic nucleus suppresses absence seizures in the rat: comparison with neurotoxic lesions. *Epilepsy Res.* **31**(1), 39–46 (1998)
 47. Fan, D., Wang, Z., Wang, Q.: Optimal control of directional deep brain stimulation in the parkinsonian neuronal network. *Commun. Nonlinear Sci. Numer. Simul.* **36**, 219–237 (2016)
 48. Chen, M., Guo, D., Wang, T., et al.: Bidirectional control of absence seizures by the basal ganglia: a computational evidence. *PLoS Comput. Biol.* **10**(3), e1003495 (2014)
 49. Chen, M., Guo, D., Li, M., et al.: Critical roles of the direct GABAergic pallido-cortical pathway in controlling absence seizures. *PLoS Comput. Biol.* **11**(10), e1004539 (2015)
 50. Lewis, L.D., Voigts, J., Flores, F.J., Schmitt, L.I., Wilson, M.A., Halassa, M.M., Brown, E.N.: Thalamic reticular nucleus induces fast and local modulation of arousal state. *Elife* **13**(4), e08760 (2015)
 51. John, Y.J., Zikopoulos, B., Bullock, D., Barbas, H.: The emotional gatekeeper: a computational model of attentional selection and suppression through the pathway from the amygdala to the inhibitory thalamic reticular nucleus. *PLoS Comput. Biol.* **12**(2), e1004722 (2016)
 52. Perry, M.S., Duchowny, M.: Surgical versus medical treatment for refractory epilepsy: outcomes beyond seizure control. *Epilepsia* **54**(12), 2060–2070 (2013)
 53. Irimia, A., Van Horn, J.D.: Epileptogenic focus localization in treatment-resistant post-traumatic epilepsy. *J. Clin. Neurosci.* **22**(4), 627–631 (2015)
 54. Fan, D., Wang, Q.: Improved control effect of absence seizures by autaptic connections to the subthalamic nucleus. *Phys. Rev. E* **98**(5), 052414 (2018)
 55. Liang, S., Wang, Z.H.: Controlling a neuron by stimulating a coupled neuron. *Appl. Math. Mech. Engl. Ed.* **40**(1), 13–24 (2019)

Publisher's Note Springer Nature remains neutral with regard to jurisdictional claims in published maps and institutional affiliations.